Modulation scheme for the bidirectional operation of the Phase Shift Full Bridge Power Converter

Manuel Escudero (1), David Meneses (1),

Noel Rodriguez (2), Diego Pedro Morales (2),

(1) Infineon Technologies Austria AG, Austria

(2) Department of Electronics and Computer Technology, University of Granada, Spain

Corresponding Author: Manuel Escudero, Infineon Technologies Austria AG, Siemenstrasse 2, 9500 Villach, Austria E-Mail: Manuel.EscuderoRodriguez@infineon.com

Telephone: +43 (0) 676 82051310

This submission is intended for the IEEE Transactions on Power Electronics

<u>This paper has never been presented at any conference or previously submitted elsewhere.</u>

***Abstract*—This paper proposes a novel modulation technique for the bidirectional operation of the Phase Shift Full Bridge (PSFB) DC/DC power converter. The forward or buck operation of this topology is well known and widely used in medium to high power DC to DC converter applications. In contrast, backward or boost operation is less typical since it exhibits large drain voltage overshoot in devices located at the secondary or current-fed side; a known problem in isolated boost converters. For that reason other topologies of symmetric configuration are preferred in bidirectional applications, like CLLC resonant converter or Dual Active Bridge (DAB). In this work, we propose a modulation technique overcoming the drain voltage overshoot of the isolated boost converter at the secondary or current-fed side, without additional components other than the ones in a standard PSFB and still achieving full or nearly full ZVS in the primary or voltage-fed side along all the load range of the converter. The proposed modulation has been tested in a bidirectional 3.3 kW PSFB with 400 V input and 54.5 V output, achieving a 98 % of peak efficiency in buck mode and 97.5 % in boost mode operation. This demonstrates that the PSFB converter may become a relatively simple and efficient topology for bidirectional DC to DC converter applications.**

***Index Terms*—Phase Shift Full Bridge, modulation technique, Bidirectional Converter, Isolated Boost Converter, Soft Switching.**

I. INTRODUCTION

Bidirectional converters are commonly used in uninterrupted power supplies (UPS) and battery energy storage systems where charging and discharging functionalities are desired to be integrated to reduce volume and cost. UPS converters are usually AC/DC converters composed of two stages: a lousy regulated AC/DC first stage, providing power factor correction (PFC), and a tightly regulated DC/DC second stage providing isolation and battery management [1]. Other applications like on board chargers are in general designed with bidirectional capability only on the DC/DC stage: they charge the battery from an AC/DC source and transfer energy from the battery to the motor, other car systems or back to the grid [2][3]. Further examples of bidirectional converter applications are found in battery manufacturing processes where batteries are charged and partially discharged for testing: a bidirectional DC/DC converter can reuse the discharging energy to charge up other batteries, saving energy and costs [4].

Commonly used DC/DC topologies as bidirectional converters are symmetric in their design and operation in forward (here referred as the charge of a battery, or buck mode operation) and reverse mode (here referred as discharge of a battery, or boost mode operation). This might seem logic or more straightforward for the designer as the converter operates basically on the same manner when working in forward and reverse directions. However, this is achieved at the expense of added complexity, design compromises and normally a negative impact on converter performance (lower efficiency than single direction converters). That is the case of Dual Active Bridge (DAB), LLC or CLLC resonant converters [5][6][7][8]. Despite the Phase Shift Full Bridge (PSFB) converter is not a symmetric bidirectional converter, it is a known alternative, but often excluded from comparative evaluations [9] due to the intrinsic problems of isolated boost converters: their high drain voltage overshoot on the secondary or current-fed side devices and the lack of ZVS capability on the primary or voltage-fed side devices. Here, in this work, we propose a novel modulation scheme for PSFB as a bidirectional converter that overcomes its drawbacks working as isolated boost converter and does so without additional circuitry, complexity, design tradeoffs or any impact on the forward operation performance.

II. OPERATION PRINCIPLES

PSFB is an isolated DC/DC buck-derived converter topology that comprises a primary side full bridge at the input (identified here by Q_1, Q_2, Q_3 and Q_4 devices, Fig. 1), an isolation transformer, a rectification stage (identified here by Q_5, Q_6, Q_7 and Q_8 devices) and an output filter (LC filter: L_o and C_o). The rectification stage may have different configurations: center tapped, current doubler or full bridge; each of them having its advantages in different applications: low voltage, high current or high voltage outputs respectively [10]; however these alternatives have no mayor impact on the working principles of the converter.

A. STANDARD (FORWARD/BUCK) OPERATION

In the standard or most commonly used modulation scheme for PSFB, the primary side bridge is controlled by two complementary pulse width modulated (PWM) signals with fixed frequency and duty cycle. The duty of the PWM signals is nearly 50 %, excluding dead times to avoid cross conduction in stacked devices (bridge leg Q_1-Q_2 and bridge leg Q_3-Q_4). A phase delay between the two PWM signals defines the voltage-time window or effective duty cycle of the main transformer (T_r). The voltage applied to the transformer is then a symmetric three level square wave which is subsequently rectified and filtered in the secondary side of the converter. The rectification stage could be passive (diode based) or active (synchronous rectification), but again, it has no mayor impact on the working principles. However, to be used as bidirectional converter, the rectification stage should be capable of active rectification.

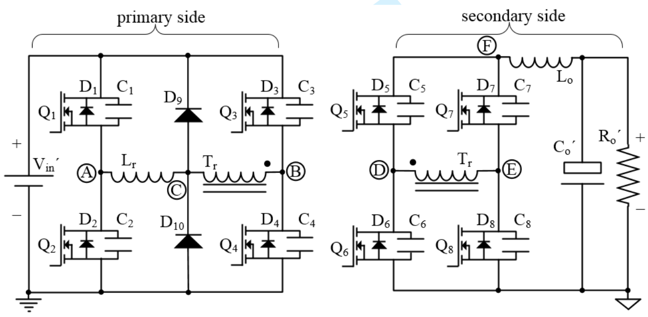

Fig. 1: Conventional Phase Shift Full Bridge DC/DC converter configuration with full bridge rectification and primary side clamping diodes.

The main characteristic of the PSFB is the harnessing of the energy in the primary and secondary inductances to reach Zero Voltage Switching (ZVS) for the primary side devices. An optimized PSFB design would ideally work in full or nearly full ZVS along all load range of the converter for the best efficiency, especially at light and medium loads, where the switching losses might be dominant [11][12]. This requires minimizing the output capacitance of the primary side devices or maximizing the available resonant energy in one or several of these ways:

- Increasing L_r. However this limits the effective duty cycle, limits the input voltage range, and could increase the drain voltage overshoot in the secondary side rectifiers.

- Decreasing the transformer magnetizing inductance (L_m). Also increases the current circulating in the primary side and, in consequence, conduction losses.
- Increasing L_o. It has only effect in one of the primary side bridge legs, which already achieves full ZVS easily in down conversion designs (reflected L_o is proportional to the square of transformer turns ratio).

Among the previous alternatives, the most commonly accepted way of increasing performance, when possible, is the usage of an external resonant inductance (L_r) right dimensioned to reach the maximum power of the converter at the minimum specified input voltage [11][12]. The induced secondary side overshoot by external L_r can be effectively reduced by the usage of primary side clamping diodes as is suggested in [14]. On the other hand, the secondary side devices are hard commutated and exhibit higher switching losses than in fully resonant converters (LLC) [12].

The previous description conforms, in summary, a standard PSFB converter as in Figure 1 that would be used to demonstrate and exemplify the bidirectional operation of the topology. It follows, however, that the proposed solution could be applied to other PSFB alternative configurations.

B. BOOST OPERATION

The PSFB converter, when working in reverse direction, transfers power from the secondary side to the primary side (as referred here), and operates as a current-fed isolated boost converter. The output filter inductance, L_o, becomes now the boost inductor in this operation mode.

The energy is stored in L_o when the secondary or current-fed side devices effectively short it between ground and the energy supply, a battery in the intended application, as in Figure 2. The energy is transferred when one of the diagonals in the current-fed side turns off, so the current is forced through the transformer and reflected into the primary side. During the next power transfer stage, the current-fed side devices may alternate operation (turning off the other diagonal) as to excite the transformer with reverse polarity generating a symmetric three level square wave that resets the transformer core flux (as in the forward working mode of the converter), to get a better core utilization and avoid saturation.

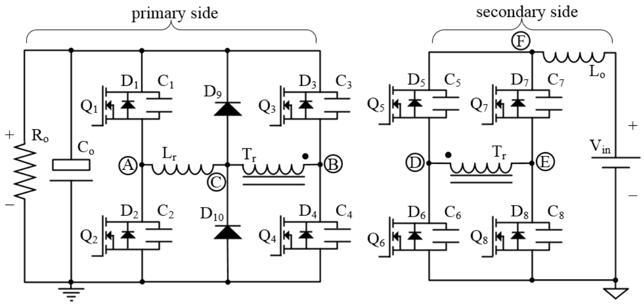

Fig. 2: Conventional Phase Shift Full Bridge working as isolated boost converter.

The primary or voltage-fed side of the converter acts now as the rectification stage when working in boost mode. The voltage-fed devices could be used as pure diode rectifiers, taking advantage intrinsic body diode of the devices, or by mounting parallel diodes whenever the devices do not have intrinsic body diode or its characteristics makes them not appropriated for diode operation (case of Wide Band-Gap devices) [15][16]. Nevertheless, if the primary side operates in diode mode, performance of the converter will be poor because of three main reasons:

- High conduction losses, even though the primary side operates with high voltage and low current levels for the intended application.
- High switching losses due to reverse recovery (Q_{rr}) and output capacitance (Q_{oss}) loss, even though PSFB converters usually mount devices with low or virtually no Q_{rr} (Schottky, SiC diodes or "fast body diode" MOSFETs) [17].
- High secondary side drain voltage overshoot at the start of the power transfer that increases electromagnetic interference (EMI). This could compromise the reliability of the converter forcing to use devices of a high voltage class with the consequent increase on the converter losses.

As it is well known, an increase in voltage breakdown of semiconductor devices has a negative impact on their figure of merit (FOM). Most widely used FOM in MOSFETs traditionally compares the *on* resistance ($R_{ds(ON)}$) and the gate charge (Q_g) since this is historically an indicative of the amount of conduction and switching losses for a specific technology or device [18].

1) SYNCHRONOUS RECTIFIERS DRAIN VOLTAGE OVERSHOOT

In the conventional boost operation, when a power transfer starts, one of the diagonals on the secondary (current-fed) bridge turns off and the primary side becomes effectively connected in series to the boost inductor L_o. A simplified equivalent circuit of this situation is presented in Fig. 3, with $i_{Lo''}$ being the primary side reflected current of L_o and i_{Lr} the current flowing through primary side resonant inductance. If $i_{Lo''}$ is greater than zero (which would be the case when operating in boost mode) and i_{Lr} is lower than $i_{Lo''}$, it will necessarily induce a voltage in V_{CA} high enough to force the current through L_r to increase until both currents $i_{Lo''}$ and i_{Lr} match. The voltage overshoot on the blocking current-fed devices is directly related to the inductance values (L_r, L_o, L_{lkg}), the stored energy (current) and output capacitance of devices (C_5, C_6, C_7, C_8).

In the PSFB converter configuration of this document D_9, D_{10} work as clamping diodes when operating in forward or buck mode. When operating in boost mode, the above mentioned induced overshoot provoked by L_r, would be effectively snubbed by D_9 or D_{10} (which one conducts depends on the secondary side switches configuration and the transformer reflected voltage polarity) and the energy would be transferred to the output of the converter (R_o, C_o). In this scenario the majority of current will pass through D_9 and D_{10} as it becomes the lowest impedance path; and as D_9 and D_{10} are intended to be clamping diodes, their conduction and switching performance would be poor. Moreover, the induced overshoot by L_{lkg} and other parasitic inductances of the circuit (L_{stray}) cannot be clamped by this technique, as there is no possibility of accessing node E´´ in real practical applications.

An obvious solution to remove the inductances causing the overshoot could include:

- Realizing a transformer with zero or nearly zero leakage, impractical in real applications.
- Removing L_o, turns the converter in fully symmetric, then known in the literature as DAB. However, this does not come for free. This approach increases rms currents through the converter and the current ripple of components with its negative effects in performance and cost. It also has a limited ZVS range capability [9].

Another possible solution consist in using secondary side snubbers as suggested in [19], at the expense of increased complexity and cost and still having a negative impact on performance (low efficiency). A modulation scheme for bidirectional operation of PSFB that overcomes current-fed voltage overshoot has already been reported in the literature [20], achieving Zero Current Switching (ZCS) in the primary side HV bridge. However, it fails to realize ZVS which is much more convenient than ZCS for modern HV silicon based devices (Super Junction MOSFETs)

[21]. In [22] another alternative modulation scheme is proposed but it can achieve ZVS in HV primary side devices only in a limited load range.

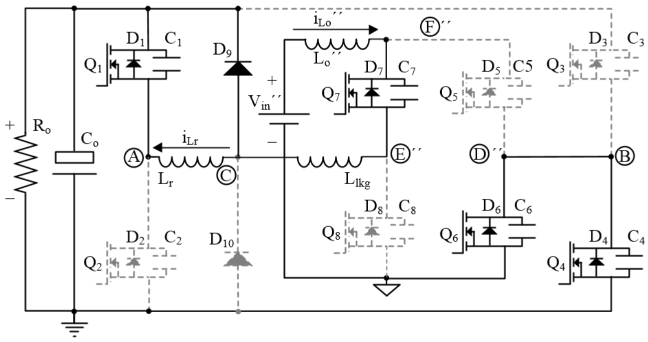

Fig. 3: Equivalent configuration of the Phase Shift Full Bridge during a power transfer as an isolated boost converter.

The proposal in this work solves the previous issues by introducing a novel modulation scheme for bidirectional operation of PSFB that overcomes the secondary side induced overshoot on a standard converter configuration (Figure 2) without affecting the forward operation performance, nor including additional circuit complexity or additional cost and still achieves full or nearly full ZVS in the voltage-fed side devices (HV bridge) along all load range.

2) PRECHARGE OF PRIMARY INDUCTANCES

The core idea of the proposed modulation scheme is to increase the current through L_r and L_{lkg} in the primary side of the converter prior to a power transfer up to the level of the reflected secondary side L_o current. In this manner, the coupling of currents at the start of a power transfer occurs effectively with no induced voltage stress, and likely with better performance: the lowest impedance path for the current flow is now through L_r and the active devices Q_1 and Q_4; the clamping diodes D_9, D_{10} conduction and switching losses are also reduced.

The current through L_r, L_{lkg} would increase when one of the diagonals in the primary side bridge is active (Q_1 and Q_4, or Q_2 and Q_3) while the transformer is effectively shorted by the secondary side devices (which is the case during the charge of the boost inductor L_o, or boost duty). In consequence, the maximum available "precharging" time of L_r, L_{lkg} corresponds to the boost duty time. The time required to raise L_r, L_{lkg} current can be estimated by Eq. (4) and the calculation can be easily implemented in a controller measuring the L_o current and the V_o voltage. This constrains to the minimum output to input voltage ratio required to operate by the relation (5).

$$Precharge_T = \frac{(L_r + L_{lkg}) \cdot I_{Lo''}}{V_o} \qquad (4)$$

$$Precharge_T \leq \frac{(V_o - V_{in''})}{V_o} \cdot T \qquad (5)$$

It follows that the proposed modulation scheme requires Q_1-Q_4 to be active devices and C_o (Figure 3) to store energy enough to raise the current through L_r and L_{lkg} up to the required level in the available time every switching period, T.

III. MODULATION SCHEME

Figure 4 shows main driving signals and waveforms of a standard modulation scheme for PSFB in T_r-lead (L_r connected between transformer and leading leg Q_1 and Q_2) [14] configuration with clamping diodes exemplified as in Fig. 1. In the Figure, the converter is operating at a load point where output filter is in CCM and the secondary side rectifiers are working as active switches. Freewheeling time [t_2-t_4] is relatively long as it is the case for practical designs where the converter has to be able to regulate on a wide input range during hold-up time conditions. Currents through L_r (i_{Lr}) and through the transformer T_r (i_{Tr}) differ due to the action of the clamping diodes D_9, D_{10} that snub the resonance between L_r and the secondary side rectifiers output capacitance at the start and at the end of a power transfer ([t_1] and [t_3]).

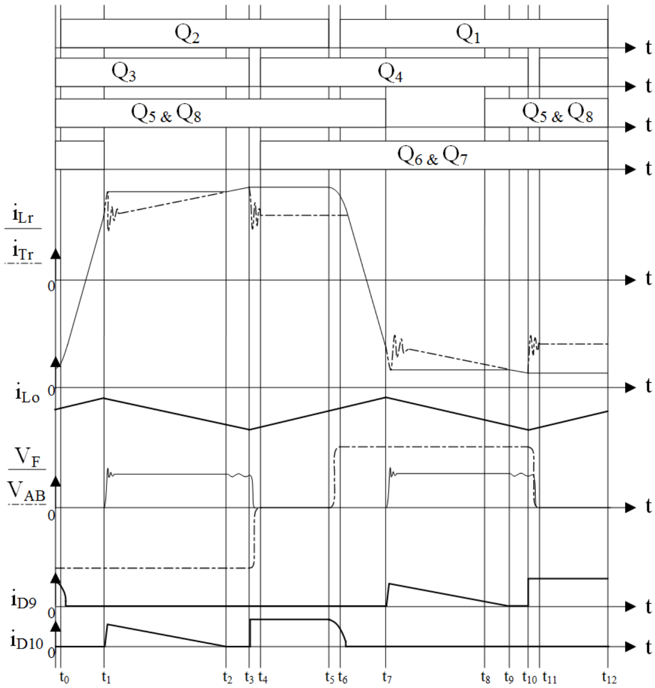

Fig. 4: Main signals scheme in the circuit for the proposed forward operation of the PSFB

Figure 5 shows the main driving signals and waveforms for the proposed modulation scheme in the reverse operation of a standard PSFB. The reader may notice the quasi-specular symmetry between Fig. 4 and Fig. 5 waveforms.

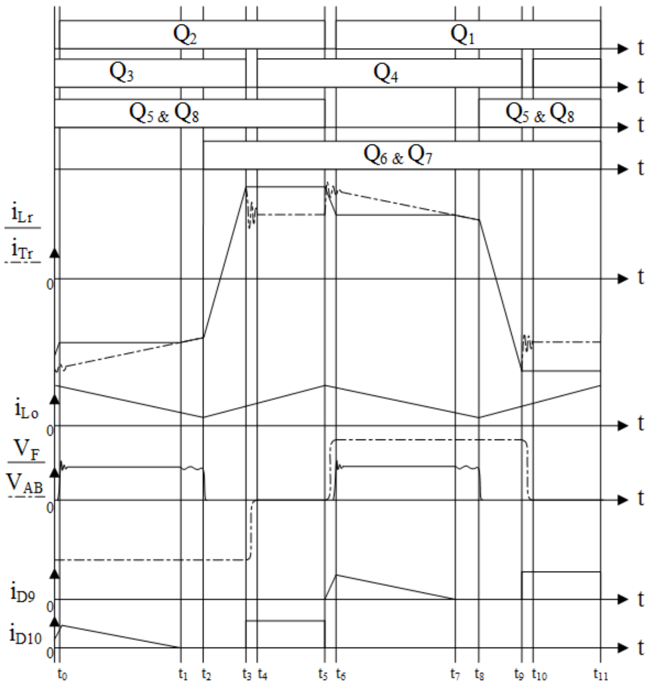

Fig. 5: Main signals scheme in the circuit for the proposed reverse operation of the PSFB

Here we analyze in the following the operation principle for the proposed reverse operation of PSFB. Before the analysis some assumptions are made: 1) all diodes and switches are ideal; 2) all switches are MOSFETs with intrinsic anti-parallel body diode 3) all capacitors and inductors are ideal 4) C_1=C_2=C_3=C_4, C_5=C_6=C_7=C_8.

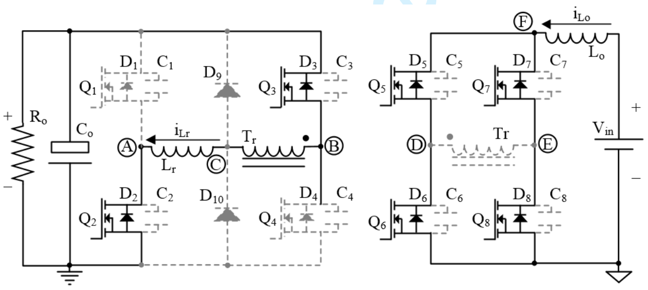

(a) [t_2, t_3]

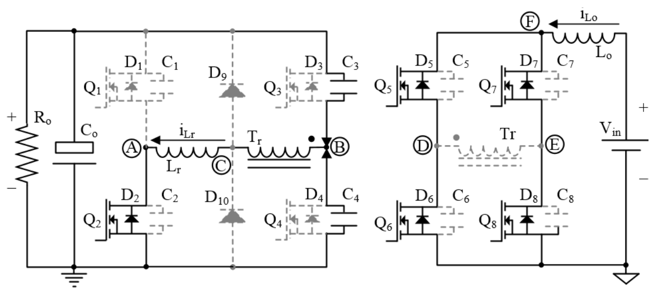

(b) [t_3]

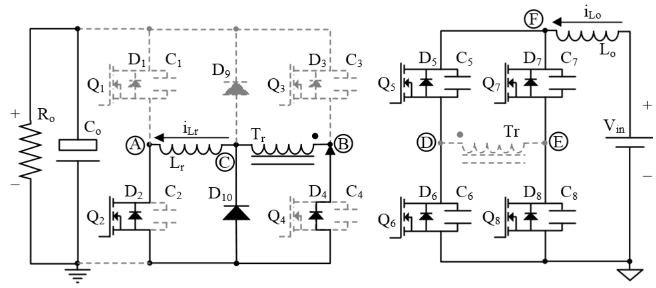

(c) [t_3, t_4]

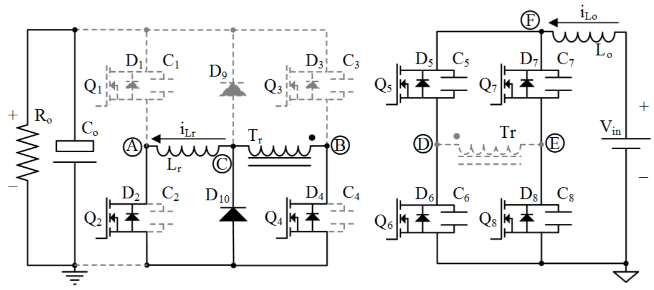

(d) [t_4, t_5]

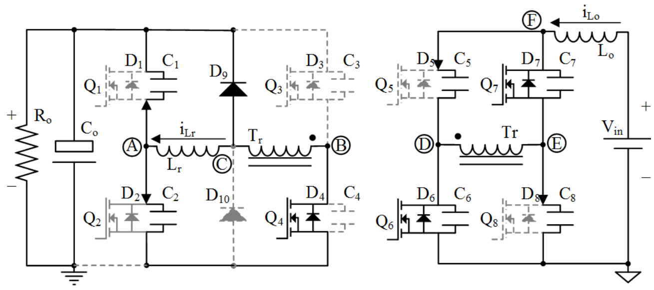

(e) [t_5]

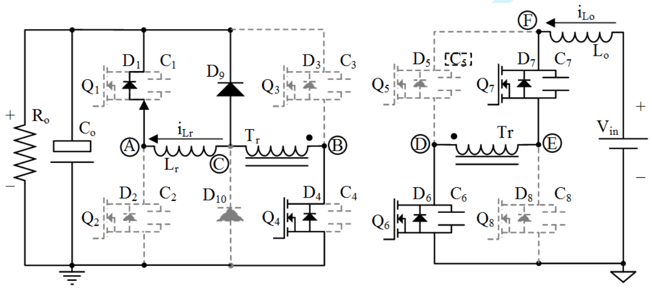

(f) [t_5, t_6]

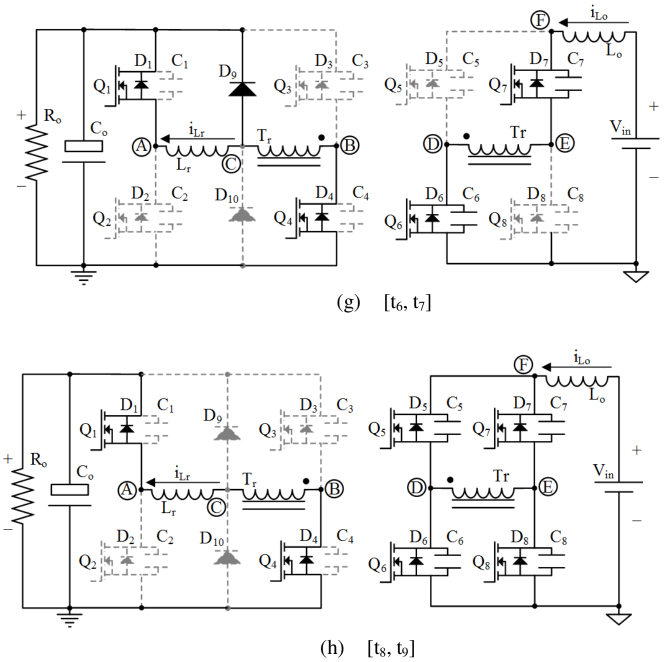

Fig. 6: Main operation modes for the proposed reverse operation of the PSFB

1) Mode 1[t_2, t_3] [Figure 6(a)]: During the interval [t_2, t_5] L_o is shorted to ground by the secondary side switches (Q_5-Q_8) and the primary side of the converter is effectively decoupled from the secondary as the transformer is also shorted.

The primary side switches Q_2 and Q_3 are turned on so the voltage at the output of the converter is applied between points A and B (V_{AB}). Since the transformer is virtually shorted all the primary voltage is applied to L_r and to L_m, and L_{lkg} of the transformer. The current through L_r and L_{lkg} reverses polarity and increases near or above the value of the reflected secondary current. At that point, the controller turns off Q_3 and stops here the so called precharging stage. This precharging stage is one of the key differences with the conventional PSFB in boost operation.

2) Mode 2[t_3] [Figure 6(b)]: Q_3 turns off and the current through L_r, L_{lkg} and L_m of the transformer starts to charge the output capacitance of switch Q_3 and discharge the output capacitance of Q_4. The current through the transformer and the leakage of transformer i_{Tr} drops since part of its energy is used for the ZVS transition of Q_3 and Q_4.
Due to the clamping diodes, the current through L_r remains nearly constant during [t_3, t_5], dismissing the effect of the clamping diode forward voltage drop and ohmic losses of the recirculation path.

3) Mode 3[t_3, t_4] [Figure 6(c)]: After the output capacitance of Q_3 is fully charged and the output capacitance of Q_4 is fully discharged (whenever there was enough energy in L_{lgk}, L_r and L_m prior to [t_3]) the intrinsic body diode of Q_4 will become forward biased and starts conducting. At this point Q_4 turns on in partial or full ZVS (depending on the balance of energies).

The current difference between i_{Lr} and i_{Tr} passes through one of the clamping diodes, D_{10} during this stage and until [t_5].

4) Mode 4[t_4, t_5] [Figure 6(d)]: The primary side current freewheels through Q_2 and Q_4. The transformer is still effectively shorted by the secondary side switches and i_{Lr} and i_{Tr} remain constant, dismissing conduction losses. The current through L_o keeps rising as it remains shorted between V_{in} and ground.

5) Mode 5[t_5] [Figure 6(e)]: End of boost inductor charging stage. Q_5 and Q_8 turn off and only one of the secondary side branches remains on. The secondary side transformer voltage V_{ED} starts to raise as Q_5 and Q_8 output capacitances are charged up by L_o.

At the same time the primary side device Q_2 turns off. The output capacitance of Q_1 will be discharged and the output capacitance of Q_2 charged by the stored energy in L_r, L_m, L_{lkg}, and, in this stage, aided also by L_o, as the primary is no longer decoupled from the secondary. L_r current drops since part of its energy is used in the ZVS transition of Q_1 and Q_2. However i_{Tr} rises up to the L_o primary reflected current. The difference between i_{Lr} and i_{Tr} continues passing through D_9. It follows that the clamping diodes conduct two times per power transfer (or four times per period) in reverse mode operation when using T_r-lead configuration as they do in buck mode operation [14].

6) Mode 6[t_5, t_6] [Figure 6(f)]: The output capacitances of Q_2 and Q_1 continue to be charged-discharged until the intrinsic body diode of Q_2 becomes forward biased and conducts (whenever there was enough energy stored in the inductances prior to [t_5]). Full ZVS during this transition is easier to be reached than during the transitions of Q_3 and

Q_4 as the energy in L_o also contributes to the resonant transition. At [t_6], Q_1 turns on in partial or full ZVS and the power transfer stage starts.

7) Mode 7[t_6, t_7] [Figure 6(g)]: The power transfer from the secondary to the primary continues. The L_r current remains nearly constant, aside from conduction losses. The T_r current follows the reflected L_o current and drops with a slope given by V_{in}, V_o, L_o and the transformer turns ratio n.

At [t_7] i_{Tr} decreases down to i_{Lr} and D_9 stops conducting. From the inspection of the voltage waveform of V_F after [t_7], it can be seen that V_C and V_F are no longer clamped: the output capacitance of Q_5 and Q_8 resonates with L_{lkg} and L_{stray} during [t_7, t_8].

8) Mode 8[t_8, t_9] [Figure 6(h)]: At [t_8] the power transfer ends and starts a new sequence of precharging the primary side inductances and charging the boost inductor.

At [t_8] Q_5 and Q_8 are hard switched turned on forcing L_o and the secondary side of the transformer to be shorted to the secondary ground. This switching loss contribution does not exist in buck operation where the secondary side devices are soft switched. However, the primary side devices can operate under full or nearly full ZVS along all load range.

The sequence repeats again starting from Mode 1 in a similar manner but now reversing polarity of the current and voltages applied to the transformer. The keen reader may observe in Figure 5 the pulse pattern applied and the waveforms for the above described sequence and the one with alternate polarity. The reader may also notice that the primary side leg transitioning after a power transfer in buck mode (also known as leading leg) becomes the leg transitioning before a power transfer in boost mode (also known as the lagging leg) with the proposed modulation scheme. This is an important difference, as it is not rare to design PSFB converters with different devices in Q_1, Q_2, Q_3, and Q_4 to account for the different available energies in the leading and lagging leg transitions. The recommendation here, for bidirectional operation, is to have the same type of devices within the primary side bridge.

B. TRANSITION BETWEEN OPERATING MODES

The transition from forward to reverse and from reverse to forward working modes of the proposed bidirectional PSFB is possible without interruption of power flow or control signals. This has already been reported in the literature as an unexpected bidirectional operation of standard PSFB when operating in forward mode, with the output filter working in forced continuous conduction mode (CCM) and the converter connected in parallel to other units [23].

The comparison of Figure 4 and Figure 5 side by side shows noticeable similitudes between both pulse patterns and the converter waveforms: for example, the primary side currents (i_{Lr}, i_{Tr}) in reverse operation mode are almost the mirror image along ordinates axis of the forward operation mode. Here we analyze how the signals change between operation modes and possible ways to transition from forward to reverse operation without stopping the converter, starting from the standard modulation of PSFB in Figure 4 and ending up in the proposed modulation scheme in Figure 5:

1. Q_5 & Q_8 turn off point will shift left in time to the turning off point of Q_2, increasing the delay between the gate and drain voltage raise of V_F (body diode conduction time) in forward working mode.
2. Q_6 & Q_7 turn on point will shift left in time starting to overlap with what was a power transfer in forward working mode. The overlap will induce a fast increase of the primary side current only limited by L_r and L_{lkg} (referred in this work as precharge time in the reverse working mode).
3. Q_6 & Q_7 turn on point will continue shifting left in time to increase the time in which the secondary side L_o is shorted to ground and i_{Lo} to shift direction, behaving then as a boost inductor.
4. Q_3 turn off point will shift to the right or to the left until reaching the required estimated precharging time in reverse working mode. Q_3 turning off point will be referenced hereafter to Q_6 & Q_7 turning on point plus the calculated precharging time. The Q_6 & Q_7 turning on point, referenced to the Q_5 & Q_8 turning off point, is now the manipulated variable of control (boost duty time).

Note that in boost operation mode, it is in fact required that before being able to turn off the current-fed bridge, the converter must change back to forward operation. In boost mode, the current through L_o flows against the intrinsic body diodes of the secondary side switches. If all the secondary side devices were turned off while the current is still flowing in reverse direction, the energy stored in L_o would resonate against their output capacitances with the consequent drain voltage overshoot. Since the output capacitance of the devices is relatively small (C_5, C_6, C_7, C_8) in relation to L_o the voltage will most likely rise above the breakdown limit and, at that point, the voltage would be clamped and the energy dissipated in the switches (with the consequent risk of damage when there is no other countermeasures).

C. SOFT START

By the nature of boost converters, the voltage at the output capacitance (C_o) has to be at least equal or higher than the voltage at the input (reflected V_{in} or $V_{in\sim}$), otherwise the current through the boost inductor (L_o) cannot be controlled (phenomenon commonly known as in-rush current). In-rush current is normally addressed in non-isolated boost converters through parallel negative temperature coefficient (NTC) thermistors and in-rush diodes that charge up the bulk capacitor prior to starting the converter to work. However, in isolated boost converters a more elaborated solution is required. When the bidirectional PSFB is part of a full AC/DC two stage converter, it would be possible to integrate the charging up of the bulk capacitance from the AC/DC stage whenever the AC grid voltage is present, as it could be the case in photovoltaic applications. Some other alternatives have been proposed in the literature [23][24].

As mentioned before, the minimum bulk voltage is also constrained by (5) for the proposed modulation scheme. In summary, a cold start of the proposed converter in reverse operation is in principle not possible without additional auxiliary circuitry or techniques [25]. Those matters are out of the scope of this work.

IV. EXPERIMENTAL RESULTS

A. DESIGN OF THE CONVERTER

A bidirectional 3300 W DC/DC PSFB converter was designed and built to test the proposed modulation scheme under the context of this work with the specifications in Table 1 for buck mode operation and the specifications in Table 2 for boost mode operation. Table 3 and Table 4 summarize of the main converter components.

TABLE I
KEY PARAMETERS OF PROTOTYPE (BUCK MODE)

Parameter	Value
Nominal input voltage	400 V
Input voltage range	360 V - 410 V
Nominal output voltage	54.5 V
Output voltage range	43 V - 60 V
Maximum output power	3300 W
Maximum output current	85 A
Peak efficiency (50% load)	97.94 %
Full load efficiency (100% load)	97.36 %
Height of the converter	1 U

TABLE II
KEY PARAMETERS OF PROTOTYPE (BOOST MODE)

Parameter	Value
Nominal input voltage	51 V
Maximum input voltage	57 V
Minimum input voltage	43 V
Nominal output voltage	400 V
Maximum output power	3300 W
Maximum output current	8.25 A
Height of the converter	1 U

TABLE III
SI MOSFETS AND DIODES

	IPL60R075CFD7	BSC093N15NS5	IDP08E65D1
V_{ds}	600 V	150 V	650 V
$R_{ds(on),max}$	75 mΩ @ 25 °C 149 mΩ @ 150 °C	9.3 mΩ @ 25 °C 14 mΩ @ 100 °C	
I_D	33 A @ 25 °C 21 A @ 100 °C	87 A @ 25 °C 55 A @ 100 °C	16 A @ 25 °C 8 A @ 100 °C
$C_{oss(er)}$	96 pF	604 pF	
$C_{oss(tr)}$	990 pF	604 pF	
$R_{G(int)}$	5.9 Ω	0.9 Ω	
V_f	1 V	0.88 V	1.35 V
Q_{rr}	570 nC	58 nC	200 nC
Q_g	67 nC	33 nC	

TABLE IV
MAGNETIC CORE SELECTION

	Core	Material	Manufacturer
Transformer	PQI 35/28	DMR95	DMEGC
L_r	PQI 35/28	DMR95	DMEGC
L_o	Toroid	HP 60 µ	CHANG SUNG

B. OVERALL LOSS ESTIMATION COMPARISON

Table 4 shows a summary of the overall estimation of losses of the converter operating in forward mode for the main points of interest in the application: 20 %, 50 % and 100 % load.

TABLE IV
3300 W FORWARD PSFB

Loss contribution	100% power	50% power	20% power
Auxiliary circuitry	1.02 W	1.02 W	1.02 W
Fan	4.91 W	0.64 W	0.64 W
Transformer core	3.32 W	3.32 W	3.32 W
Transformer conduction	26.11 W	7.39 W	2.02 W
Lr core	0.48 W	0.23 W	0.07 W
Lr conduction	2.03 W	0.53 W	0.11 W
Lo core	0.67 W	0.67 W	0.67 W
Lo conduction	4.55 W	1.10 W	0.18 W
Primary bridge conduction	11.81 W	2.81 W	0.58 W
Primary bridge switching	4.56 W	2.04 W	1.68 W
Primary bridge driving	0.43 W	0.43 W	0.43 W
Secondary bridge conduction	11.27 W	2.52 W	0.41 W
Secondary bridge switching	7.13 W	6.25 W	5.70 W
Secondary bridge driving	0.84 W	0.84 W	0.84 W
Snubber	0.26 W	0.26 W	0.26 W
Clamping diodes conduction	2.11 W	2.47 W	2.65 W
Capacitors	0.38 W	0.35 W	0.34 W
PCB conduction	7.60 W	1.91 W	0.32 W

Figure 7 shows the overall losses distribution of the converter operating in forward mode. The overall distribution was estimated from the measured efficiency of the real converter, thermographic captures, finite element (FEA), circuit and numeric simulations.

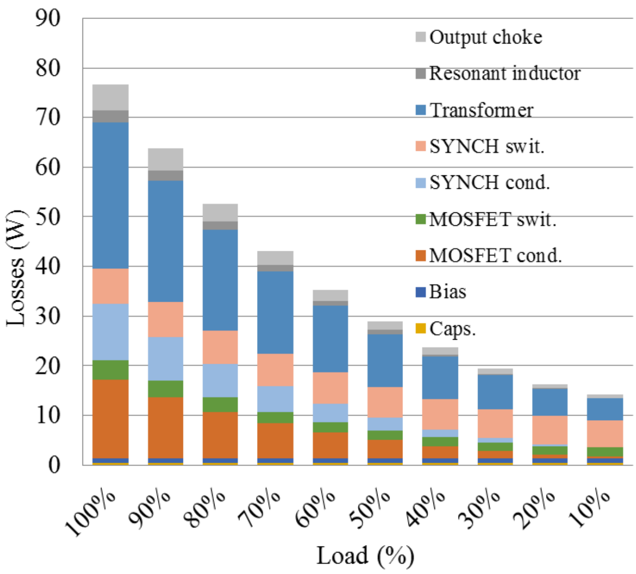

Fig. 7: Overall losses distribution of the 3300 W PSFB prototype

Based on the estimated distribution of losses, the transformer appears to be the main contributor at 50 % load point and above. This supports the hypothesis that the performance of the converter in this power and voltage class depends mostly on the design of the magnetics. When operating the converter in reverse operation mode (boost) the overall efficiency of the system is relatively lower due to the additional contribution of the clamping diodes conduction losses and the losses due to the hard switching of the secondary side devices during turn on. All other contributions to the losses are expected to remain approximately the same due to the nearly symmetric waveforms in the different operating modes.

C. WAVEFORMS

The reader can compare the experimental waveforms in Figure 8 and Figure 9 with the diagrams in Figure 4 and Figure 5 respectively for a better and more complete understanding.

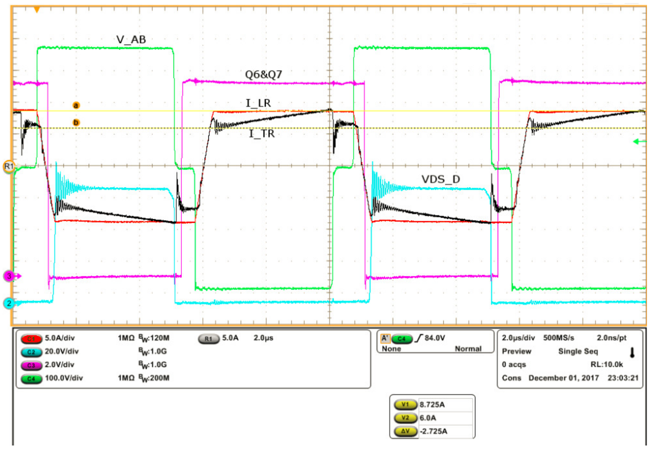

Fig. 8: Forward operation of the 3300W PSFB converter prototype.

Figure 8 captures forward operation at full load (3300 W), nominal 380 V input and 54.5 V output, approximately 61 A average output current. Some details of interest in Fig. 8:

- The primary side bridge operates in full ZVS. The gate voltage of the bridge is not captured here, but V_{AB} (green curve) shows the characteristic smooth transitions without noticeable overshoot indicative of soft switching.
- The secondary side drain voltage (blue curve) overshoot (around 95 V) is well under the breakdown limit of the devices mounted (150 V).
- The secondary side signal driving the gate (purple curve) minimizes the intrinsic diode conduction time. It reduces conduction and reverse recovery losses.
- The transformer current (black curve) accounts for the reflected output plus the magnetizing current during power transfer. In this design, the magnetizing inductance is relatively low, in the range of 650 uH, helping to achieve ZVS in HV devices at light loads.

- The difference between the transformer current and the resonance inductance current (red curve) passes through the clamping diodes D_9, D_{10} (area enclosed by red and black curves).

Figure 9 captures the boost mode operation at full load (3300 W), 54.5 V input and 400 V output leading to approximately 8.25 A average output current. Some details of interest are shown in Figure 9:

- The primary side bridge operates in ZVS. V_{AB} (pink curve) shows higher drain overshoot (432 V) than Fig. 8, however it is still well under the breakdown limit of the mounted devices (600 V). This is due to the fact that the turn off current peak seems to be higher in this operating condition (notice the change in scale of the current waveforms between Figure 8, 5 A per division, and Figure 9, 10 A per division).
- The secondary side drain voltage overshoot (red curve) is larger than in forward mode (101 V) but still well under the limit.
- The secondary side devices are hard switched during the turning on. There is no delay between the gate signals (green curve) and the drain voltage at the turn on point. A closer look at the transition shows the indicative plateau in the gate voltage.
- i_{Lr} is precharged just at the value of the reflected current at the start of the power transfer. T_r current (same as the transformer current) is slightly under that value. Experiments have revealed that there is a tradeoff between the secondary side voltage overshoot and the primary side circulating current losses.
- The clamping diodes conduct more current in comparison to forward mode. The area enclosed between i_{Tr} (black curve) and i_{Lr} (blue curve) corresponds to the current that passes through the clamping diodes, as in Figure 8.

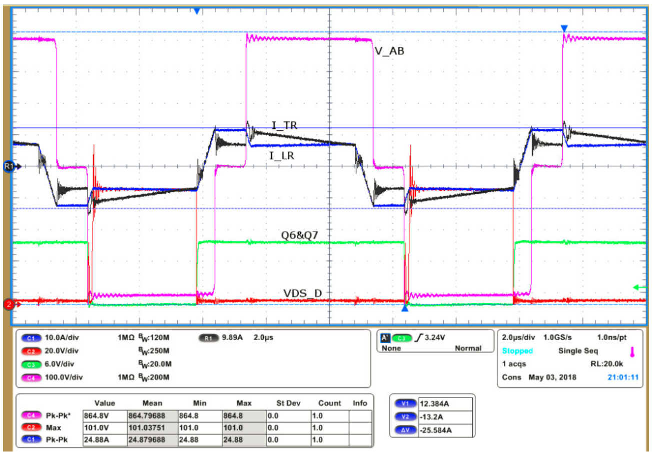

Fig. 9: Capture of the signals during reverse operation of the 3300 W PSFB prototype converter.

D. EFFICIENCY

The efficiency of the the 3300 W PSFB prototype was measured at nominal operating conditions in buck and boost operation modes. Table 5 is a summary of the testing and measurement equipment used to obtain the results in this work. Figure 10 shows the results of the efficiency measurements. As expected, the performance in reverse operation is lower than in the forward operation mode.

Due to thermal limitations of the design and the lower efficiency in reverse mode operation, the maximum steady state power that the converter could deliver was rated to 3200 W in boost mode operation for the efficiency measurements (the converter has to reach thermal equilibrium in every working point before recording the results).

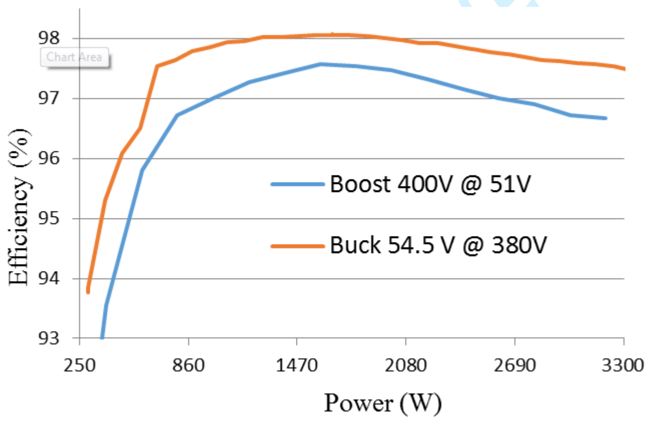

Fig. 10: Overall efficiency of the the 3300 W PSFB prototype converter operating in forward and in reverse modes. Auxiliary bias and fan were included in the measurements.

The prototype was designed to operate with forced air cooling and enclosed in a case. The thermal captures of the converter in Figure 11 and Figure 12 where taken without enclosure for illustration purposes since the case material was not transparent in the infrared spectrum. Reader may notice that the temperatures are higher in these captures than they would be when the converter operates with the proper air flow within its enclosure.

TABLE V
TESTING AND MEASURING EQUIPMENT

	Model	Manufacturer
DC supply	EA-PS 8000	Elektro-automatik
DC supply	62012P-600-8	Chroma
Electronic load	EA-ELR 9000	Elektro-automatik
Electronic load	63202	Chroma
Electronic load	63202	Chroma
Power analyzer	WT3000	Yokogawa
Scope	MSO5204B	Tektronix
Active current probe	TCP0030A	Tektronix
HV differential probe	THDP0200	Tektronix
Passive probe	TPP0100	Tektronix

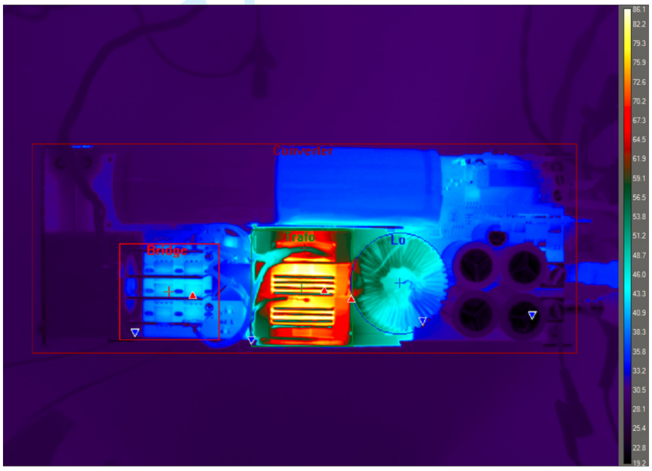

Fig. 11: Thermographic image during the forward operation of 3300W PSFB. Full load

Figure 11 shows the converter operating in forward mode at full load. The stacked magnetic structure conformed by the transformer and the resonant inductance is the hottest area in the converter. As above mentioned, the transformer is the main contributor to losses and in addition, the secondary side devices are placed right under the transformer and part of their losses will dissipate through the magnetic structure.

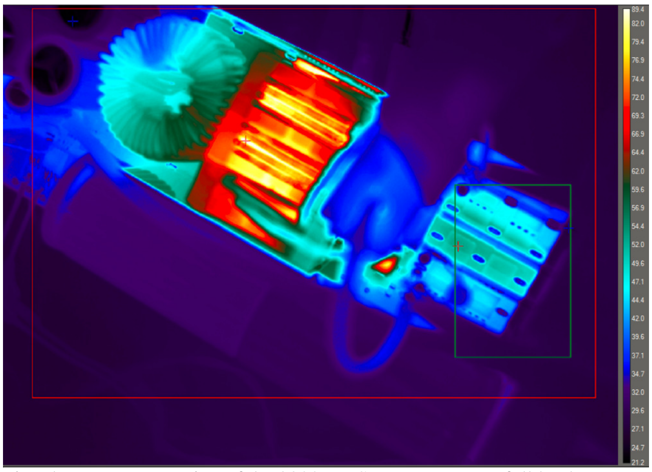

Fig. 12: Thermographic image during the reverse operation of the 3300W PSFB prototype at full load.

Figure 12 shows a top view of the converter operating in reverse mode at full load. As in Figure 11 the transformer is the hottest component and it constitutes the main contribution of losses also in boost operation mode. The reader may notice that the clamping diodes (hot spot by the right side of transformer in Fig. 12) reach higher temperature in Fig. 12 than in Fig. 11 due to above mentioned additional conduction losses.

V. CONCLUSION

In this paper a modulation scheme for the operation of the PSFB as a bidirectional DC/DC converter has been proposed to overcome well-known problems on isolated boost converters: high drain voltage overshoot on the secondary or current-fed side devices and the lack of ZVS capability on the primary or voltage-fed side devices; without penalties in complexity, cost or performance.

A high efficiency prototype of bidirectional 3300 W PSFB was designed and built to demonstrate the feasibility of the proposed solution. When working in reverse or boost mode, the high-voltage primary side devices achieve full or nearly full ZVS along all load range of the converter; however, the secondary side low-voltage devices are hard switched turned on, whereas they are soft switched in buck operation mode. The conduction losses of the primary side clamping diodes are also higher in the boost mode compared to the buck mode. The additional contribution to losses decreases the overall system efficiency of the converter when working in reverse mode in comparison to forward mode.

The prototype achieves a peak efficiency of 98.05 % in the buck mode and 97.5 % in the boost mode at nominal conditions and 50 % load point. This work demonstrates the the PSFB is a competitive alternative when building highly efficient and cost-competitive bidirectional DC/DC converters.

References

[1] M. Ryu, D. Jung, J. Baek and H. Kim, "An optimized design of bi-directional dual active bridge converter for low voltage battery charger," *2014 16th International Power Electronics and Motion Control Conference and Exposition*, Antalya, 2014, pp. 177-183.

[2] Keun-Wan Koo, Dong-Hee Kim, Dong-Gyun Woo and Byoung-Kuk Lee, "Topology comparison for 6.6kW On board charger: Performance, efficiency, and selection guideline," *2012 IEEE Vehicle Power and Propulsion Conference*, Seoul, 2012, pp. 1520-1524.

[3] Huafeng Xiao, Donghua Chen and Shaojun Xie, "A ZVS bi-directional DC-DC converter for vehicular electronics," *2005 IEEE Vehicle Power and Propulsion Conference*, Chicago, IL, 2005, pp. 7 pp.-.

[4] X. Yu and P. Yeaman, "A new high efficiency isolated bi-directional DC-DC converter for DC-bus and battery-bank interface," *2014 IEEE Applied Power Electronics Conference and Exposition - APEC 2014*, Fort Worth, TX, 2014, pp. 879-883.

[5] H. Li *et al.*, "A 6.6kW SiC bidirectional on-board charger," *2018 IEEE Applied Power Electronics Conference and Exposition (APEC)*, San Antonio, TX, 2018, pp. 1171-1178.

[6] H. Tao, A. Kotsopoulos, J. L. Duarte and M. A. M. Hendrix, "Transformer-Coupled Multiport ZVS Bidirectional DC–DC Converter With Wide Input Range," in *IEEE Transactions on Power Electronics*, vol. 23, no. 2, pp. 771-781, March 2008.

[7] A. K. Jain and R. Ayyanar, "Pwm control of dual active bridge: Comprehensive analysis and experimental verification," in *IEEE Transactions on Power Electronics*, vol. 26, no. 4, pp. 1215-1227, April 2011.

[8] A. Hillers, D. Christen and J. Biela, "Design of a Highly efficient bidirectional isolated LLC resonant converter," *2012 15th International Power Electronics and Motion Control Conference (EPE/PEMC)*, Novi Sad, 2012, pp. DS2b.13-1-DS2b.13-8.

[9] F. Krismer, J. Biela and J. W. Kolar, "A comparative evaluation of isolated bi-directional DC/DC converters with wide input and output voltage range," *Fourtieth IAS Annual Meeting. Conference Record of the 2005 Industry Applications Conference, 2005.*, Kowloon, Hong Kong, 2005, pp. 599-606 Vol. 1.

[10] Xinbo Ruan, *Soft-Switching PWM Full-Bridge Converters*. Nanjing University of Aeronautics and Astronautics, China: Wiley, 2014, pp. 1-66, 121-147, 181-198.

[11] U. Badstuebner, J. Biela and J. W. Kolar, "An optimized, 99% efficient, 5 kW, phase-shift PWM DC-DC converter for data centers and telecom applications," *The 2010 International Power Electronics Conference - ECCE ASIA -*, Sapporo, 2010, pp. 626-634.

[12] Zhao, L.; Li, H.; Liu, Y.; Li, Z. High Efficiency Variable-Frequency Full-Bridge Converter with a Load Adaptive Control Method Based on the Loss Model. *Energies* 2015, *8*, 2647-2673.

[13] R. Siemieniec, C. Mößlacher, O. Blank, M. Rösch, M. Frank and M. Hutzler, "A new power MOSFET generation designed for synchronous rectification," *Proceedings of the 2011 14th European Conference on Power Electronics and Applications*, Birmingham, 2011, pp. 1-10.

[14] Xinbo Ruan and Fuxin Liu, "An Improved ZVS PWM Full-bridge Converter with Clamping Diodes," *2004 35th Annual IEEE Power Electronics Specialists Conference* (IEEE Cat. No 04CH37551), Aachen, Germany 2004, pp. 1476-1481 Vol. 2.

[15] R. Reiner *et al*., "Integrated reverse-diodes for GaN-HEMT structures," *2015 IEEE 27th International Symposium on Power Semiconductor Devices & IC's (ISPSD)*, Hong Kong, 2015, pp. 45-48.

[16] X. Hou, D. Boroyevich and R. Burgos, "Characterization on latest-generation SiC MOSFET's body diode," *2016 IEEE 4th Workshop on Wide Bandgap Power Devices and Applications (WiPDA)*, Fayetteville, AR, 2016, pp. 247-252.

[17] L. Saro, K. Dierberger and R. Redl, "High-voltage MOSFET behavior in soft-switching converters: analysis and reliability improvements," *INTELEC - Twentieth International Telecommunications Energy Conference (Cat. No.98CH36263)*, San Francisco, CA, USA, 1998, pp. 30-40.

[18] H. Wang, F. Wang and J. Zhang, "Power Semiconductor Device Figure of Merit for High-Power-Density Converter Design Applications," in *IEEE Transactions on Electron Devices*, vol. 55, no. 1, pp. 466-470, Jan. 2008.

[19] Lizhi Zhu, Kunrong Wang, F. C. Lee and Jih-Sheng Lai, "New start-up schemes for isolated full-bridge boost converters," in *IEEE Transactions on Power Electronics*, vol. 18, no. 4, pp. 946-951, July 2003.

[20] P. Xuewei and A. K. Rathore, "Novel bidirectional snubberless soft-switching naturally clamped zero current commutated current-fed dual active bridge (CFDAB) converter for fuel cell vehicles," *2013 IEEE Energy Conversion Congress and Exposition*, Denver, CO, 2013, pp. 1894-1901.

[21] J. Wang, H. S. Chung and R. T. Li, "Characterization and Experimental Assessment of the Effects of Parasitic Elements on the MOSFET Switching Performance," in *IEEE Transactions on Power Electronics*, vol. 28, no. 1, pp. 573-590, Jan. 2013.

[22] L. Zhu, "A novel soft-commutating isolated boost full-bridge ZVS-PWM DC-DC converter for bidirectional high power applications," *2004 IEEE 35th Annual Power Electronics Specialists Conference (IEEE Cat. No.04CH37551)*, Aachen, Germany, 2004, pp. 2141-2146 Vol.3.

[23] Y. Jeong, S. Cho, D. Kim, G. Moon and C. Kim, "Unexpected bi-directional operation of Phase-Shift Full-Bridge Converter in parallel operation system," *2013 IEEE ECCE Asia Downunder*, Melbourne, VIC, 2013, pp. 999-1004.

[24] K. Lindberg-Poulsen, Z. Ouyang, G. Sen and M. A. E. Andersen, "A new method for start-up of isolated boost converters using magnetic- and winding-integration," *2012 Twenty-Seventh Annual IEEE Applied Power Electronics Conference and Exposition (APEC)*, Orlando, FL, 2012, pp. 340-345.

[25] Kunrong Wang, F. C. Lee and J. Lai, "Operation principles of bi-directional full-bridge DC/DC converter with unified soft-switching scheme and soft-starting capability," *APEC 2000. Fifteenth Annual IEEE Applied Power Electronics Conference and Exposition (Cat. No.00CH37058)*, New Orleans, LA, USA, 2000, pp. 111-118 vol.1.